

A New Baseline for GreenAI: Finding the Optimal Sub-Network via Layer and Channel Pruning

Xiaoying Zhi^{1,*}, Varun Babbar³, Pheobe Sun^{2,*} and Fran Silavong³ and Ruibo Shi³ and Sean Moran³

ETH Zurich¹

University College Dublin²

JP Morgan Chase³

xiazhi@ethz.ch, varun.babbar@jpmchase.com, wenyi.sun@ucdconnect.ie, {fran.silavong, ruibo.shi, sean.j.moran}@jpmchase.com,

Abstract

The concept of Green AI has been gaining attention within the deep learning community given the recent trend of ever larger and more complex neural network models. Some large models have billions of parameters causing the training time to take up to hundreds of GPU/TPU-days. The estimated energy consumption can be comparable to the annual total energy consumption of a standard household. Existing solutions to reduce the computational burden usually involve pruning the network parameters, however, they often create extra overhead either by iterative training and fine-tuning for static pruning or repeated computation of a dynamic pruning graph. We propose a new parameter pruning strategy that finds the effective group of lightweight sub-networks that minimizes the energy cost while maintaining comparable performances to the full network on given downstream tasks. Our proposed pruning scheme is green-oriented, such that the scheme only requires one-off training to discover the optimal static sub-networks by dynamic pruning methods. The pruning scheme consists of a lightweight, differentiable, and binarized gating module and novel loss functions to uncover sub-networks with user-defined sparsity. Our method enables pruning and training simultaneously, which saves energy in both the training and inference phases and avoids extra computational overhead from gating modules at inference time. Our results on CIFAR-10 and CIFAR-100 suggest that our scheme can remove $\approx 50\%$ of connections in deep networks with $< 1\%$ reduction in classification accuracy. Compared to other related pruning methods, our method has a lower accuracy drop for equivalent reductions in computational costs.

1 Introduction

The benefit of large, sparse, and over-parameterised models have brought significant energy cost as a sacrifice to

their state-of-the-art (SOTA) performances [Schwartz *et al.*, 2020]. For example, the vision transformer model (ViT-L16) with 307M parameters can achieve 99.42% accuracy on the CIFAR-10 dataset and 87.76% on the ImageNet dataset [Dosovitskiy *et al.*, 2020]. The training of ViT-L16 model equires 680 TPUv3-core-days¹ and 3672kWh energy consumption, equivalent to 32.5% of the annual energy consumption of an average US household [Dosovitskiy *et al.*, 2020; Jouppi *et al.*, 2020; EIA US, 2021].

Network pruning is one direction aiming at searching for greener AI models, based on the assumption that over-parameterized networks can safely remove parameters before or after training, without significantly affecting the network performances [Denil *et al.*, 2013]. There are two common types of network pruning methods – static and dynamic. Static network pruning generates a unified sub-network for all data, while dynamic pruning computes for different suitable sub-networks to different data samples. Static network pruning often requires pre-defined neuron importance measure that thresholds which trained neurons to be pruned [Shafiee *et al.*, 2018; Luo *et al.*, 2019; Cheong, 2019; Zhang and Stadie, 2019; Lin *et al.*, 2020]. Further fine-tuning or regrowing of the selected sub-network are often involved after training, which can potentially lead to further improvement in performance [Han *et al.*, 2015; Zhu *et al.*, 2021; Hou *et al.*, 2022]. Dynamic pruning, on the other hand, applies a parameterized and learnable gate function that computes the neuron importance on the fly, leading to a different computational graph for each data sample. The training phase optimizes the learnable gating functions with the empirical loss, and the inference phase computes the appropriate sub-network from gates’ forward propagation results [Veit and Belongie, 2017; Gao *et al.*, 2018; Bejnordi *et al.*, 2019; Yin *et al.*, 2021].

From a Green AI perspective, neither of the existing dynamic or static pruning approach is ideal. Dynamic pruning is not optimal for parallel computing due to necessary indexing operations at inference and causes overhead from extra connection importance computations. Static pruning can reduce computational resources at inference, but the itera-

*Work done while at JP Morgan

¹Multiplication of the number of used TPUv3 cores and the training time in days

tive pruning-and-fine-tuning process consumes more computational resources and time during the training phases. One-shot pruning after training is no better than the iterative procedure as its effectiveness heavily depends on the assumed priors, which lack verification in their validity prior to training [Lee *et al.*, 2018].

Our pruning method is able to compute for a smaller network without costing significant training resources, by simultaneously optimizing the network structure and parameters. This simultaneous optimization is realized with a *light-weight trainable binary gating module* along with *polarising regularization*. The polarising regularization allows for the emergence of a stable sub-network that performs well for all data points at the end of training. The inference time is then reduced since the static sub-network is ready-to-use. We verify the scheme’s validity on two types of pruning (layer and channel) on different ResNets [He *et al.*, 2015], applied to two differently-sized datasets (CIFAR-10 and CIFAR-100 [Krizhevsky, 2009]). Comparisons with naive baselines and previous works are also presented.

2 Related Works

2.1 Energy-Aware AI

[Schwartz *et al.*, 2020] were among the first authors to define the concepts of Green AI (environmentally friendly AI) and Red AI (heavily energy-consuming AI), and suggest that models should be evaluated beyond accuracy by taking into account their carbon emission and electricity usage, elapsed time, parameter count, and floating point operations (FPOs/FLOPs). [Patterson *et al.*, 2021] and [Dodge *et al.*, 2022] proposed frameworks to quantify the carbon emission resulting from usage of specific AI models on various common devices. In order to reduce the carbon emission from model training, different approaches have been commonly used. For example, model quantization can be used to reduce the elapsed time and processor memory usage [Gholami *et al.*, 2021], while network distillation and network pruning approaches can be used to reduce the number of parameters and total FLOPs [Hinton *et al.*, 2015].

2.2 Network Pruning

Network pruning aims to rank the importance of the edges in a neural network model in order to find a sub-network with the most important edges. There are two approaches to achieve this goal: *static* or *dynamic* methodologies. Static network pruning finds a unified sub-network at the end of the training, and is usually followed-up by a fine-tuning procedure to further improve the sub-network performance. This pruning scheme relies on the calculated importance scores of the edges of interest. The edge importance can be calculated, for example, by the magnitude or the influence of an edge to the final output.

In convolutional neural networks (CNNs), eExperiments on static feature map pruning [Li *et al.*, 2016a] and channel pruning [He *et al.*, 2017a] demonstrated a 30% reduction in FLOPs or a $2.5\times$ reduction in GPU time with only negligible performance degradation or even improvement in some cases. [Cai *et al.*, 2019] expanded the problem to multi-stage

pruning to make the pruning approach adaptable to different size requirements. This goal was achieved by training and fine-tuning the sub-networks with incremental size reduction while making sure the model accuracy stays the same each time the size requirement gets reduced.

Dynamic pruning, on the other hand, aims to find input-variant sub-networks, and. Thus input-dependent elements are usually added to the original network often adds input-variant elements to compute the importance of the edges under interest. [Veit and Belongie, 2017] [Veit and Belongie, 2017] proposed the adaptive inference graph that computes the importance of the CNN layers with a probabilistic and learnable gating module before each layer. [Lin *et al.*, 2017] proposed a similar framework to prune the CNN channels by using reinforcement learning to train an optimal channel importance scorer.

Combining both static and dynamic pruning methods can potentially achieve a greater impact on green AI. This approach can leverage static pruning’s compatibility with parallel computing, saving energy especially on GPU computation. This approach can also leverage dynamic pruning’s advantage of adaptation to different inputs by different optimal sub-network structures. [Lee, 2019], for example, proposed a sub-differentiable sparsification method where parameters can potentially be zeroed after optimization under stochastic gradient descent. However, the non-unified sub-networks still cause excess indexing computation in parallel computing. Our work focuses on the problem of finding a unified sub-network for data following a certain distribution, by using the dynamically pruned sub-networks as intermediate states.

To unify the sub-networks, some works proposed a concept of dynamic neural graph, where each neural network is represented as a graph with nodes being the variables and edges being the connections [Wortsman *et al.*, 2019]. The pruning procedure involves updating edge weights by back-propagation and selecting a fixed proportion to prune according to the weight magnitudes. In this scheme, the graph representation and corresponding pruning can cover recurrent neural networks (cyclic graphs), beyond sequential networks (acyclic graphs) as in most work. Some later research expands the methods to find sub-networks without training for edge weights, proving that randomly weighted neural networks already contain sub-networks that give satisfactory performance results [Ramanujan *et al.*, 2019].

Our findings also corroborate recent work on the existence of several ‘lottery tickets’, i.e. pruned sub-networks that can achieve similar accuracy as the original network [Frankle and Carbin, 2019]. To generate such networks, the IMP (Iterative Magnitude Pruning) scheme involves iterative pruning and training over multiple rounds until convergence. This is different from our proposed method, which performs simultaneous training and pruning in one training session and is therefore computationally cheaper to train.

2.3 Discrete Stochasticity and Gradient Estimation

To obtain a stable sub-network structure through gradient-based optimization *i.e.* binary activation statuses for each connection, a gating module is needed with differentiable and discrete latent variables. Discrete variables often requires

gradient estimation when their gradients are not directly computable.

One estimation approach is the Gumbel-Softmax (GS) estimator [Jang *et al.*, 2016], which enables differentiation in sampling categorical data from a GS distribution. Gradients *w.r.t.* the categorical output distribution is well-defined from the GS distribution. This technique is often applied to generative models for sequences requiring sampling under multinomial distributions [Kusner and Hernández-Lobato, 2016; Shen *et al.*, 2021; Chang *et al.*, 2019].

A simpler approach is the straight-through estimator (STE) [Bengio *et al.*, 2013], which binarizes the stochastic output based on a threshold in the forward pass, and heuristically copies the gradient of next layer to the estimator. Experiments show that neural networks gated by the STE give the lowest error rate among other differentiable gates (multinomial and non-multinomial) [Bengio *et al.*, 2013]. More details about the STE are presented in Section *Gating Modules and Straight-through Estimator*.

2.4 Sparsity Regularizers

In the network pruning task, often a sparsity regularizer is involved to encourage the pruning ratio during training, among which l_1 - and l_2 - regularizers are two most common ones. However, standard regularization functions might lead to unnecessary pruning or mis-estimation of network connectivity importance. Regularizers that takes more network structure into consideration include $l_{2,0}$ - and $l_{2,1}$ - structured sparsity regularization [Lin *et al.*, 2019], grouped (on samples or on feature maps) sparsity regularization [Li *et al.*, 2020], etc.

[Srinivas and Babu, 2015] proposed a binarizing regularizer that encourages each network connection to approach either 1 or 0 for all samples. The binarizing idea can also be extended to continuous activation rates. For example, [Zhuang *et al.*, 2020] integrated a polarization regularizer into network pruning to force the deactivation of neurons. Networks pruned under this setting achieve the highest accuracy even at high pruning rate compared to other pruning schemes.

3 Problem Setup: Simultaneous Parameter and Architecture Learning

We denote a neural network with full connectivity in the form of a graph as $\Phi := (V, E)$, where V is a set of nodes, E is the set of edges $E := \{e^{(x,y)}, \forall x, y \in V\}$. A sub-network with partial connectivity can thus be represented as $\Phi' = (V, E')$ where $E' \subseteq E$. We also denote the transformation of a network as $f_\theta(\cdot) \equiv f(\cdot; \theta)$, where θ denotes all the parameters in a network. Each edge $e \in E$ is associated with a weight θ^e . For the full network $\theta = \theta_\Phi$, and for the sub-network $\theta = \theta_{\Phi'}$. A sub-network can be expressed in terms of a full-network using an activation matrix \mathbf{W}_e with certain elements zeroed, *i.e.*

$$\theta_{\Phi'} = \mathbf{W}_e^\top \theta_\Phi, \quad (1)$$

where $w_{e,c} \in \{0, 1\}$ for every entry in the edge activation matrix \mathbf{W}_e is binary.

In network pruning, we aim to find a sub-network Φ' and the optimal network parameters $\theta_{\Phi'}^*$ simultaneously. We estimate the optimal solution $\theta_{\Phi'}^*$ with $\hat{\theta}_{\Phi'}$ by minimising the

empirical loss, *i.e.*

$$\min_{\theta_{\Phi'}, \Phi'} \mathcal{L}(f(\mathbf{x}; \theta_{\Phi'}), \mathbf{y}). \quad (2)$$

Using the settings in Eq.1, we can safely reform the above objective as:

$$\min_{\theta_\Phi, \mathbf{W}_e} \mathcal{L}(f(\mathbf{x}; \mathbf{W}_e^\top \theta_\Phi), \mathbf{y}). \quad (3)$$

4 Methodology

In practice, the edge activation matrix \mathbf{W}_e is not learned as a whole and each entry in the matrix is not independent. When training a sequential network, the activation of former connections can affect the outputs of the later connections, and thus also affect the gradients back-propagation computations. A naive binary/categorical \mathbf{W}_e would make gradients unable to propagate back as a function of constant value has zero gradient. Therefore, a gradient estimator is needed as the core gating element of each connectivity. We choose the straight-through estimator (STE), as introduced in Section *Discrete Stochasticity and Gradient Estimation*, as this core element.

4.1 Network Architectures

Figure 1 illustrates the design for gating module integration into ResNet. Our pruning scheme has slightly different workflows for the training phase and the testing phase. In training, the gating modules with learnable dense layers are trained as part of the network. At inference (for validation or test), the resultant \mathbf{W}_e is loaded, which decides the subset of parameters to be selected – only the connections with a non-zero $w_{e,c}$ will be loaded for parameters and included in the forward pass.

The choice of ResNet as the base network is based on the necessity of residual connections under our proposed scheme to avoid potential computational path termination in the middle of the full network due to a deactivated full layer. Under the discussion of ResNet, we focus on CNN-centered layer and channel (feature map) pruning. However, we also argue that this methodology has the potential be applied to any type of connection, even in less structured pruning (*e.g.* selected kernel-to-kernel connections between convolutional layers). While our method has similarities with dropout-based methods in ResNets, these involve pruning specific connections between nodes - from an architectural standpoint this doesn't necessarily reduce the number of FLOPs unless

4.2 Straight-through Estimator

We chose Straight-through estimator (STE) as the binary head for the gating module. The forward path of STE is a hard thresholding function:

$$STE(x) = \begin{cases} 1, & \text{if } x > 0 \\ 0, & \text{if } x \leq 0 \end{cases}. \quad (4)$$

The backward gradient reflects why it's named as 'straight-through':

$$\frac{\partial \mathcal{L}}{\partial x} = \frac{\partial \mathcal{L}}{\partial STE(x)} \cdot \frac{\partial STE(x)}{\partial x} = \begin{cases} \frac{\partial \mathcal{L}}{\partial STE(x)}, & \text{if } |x| \leq 1 \\ 0, & \text{if } |x| > 1 \end{cases}, \quad (5)$$

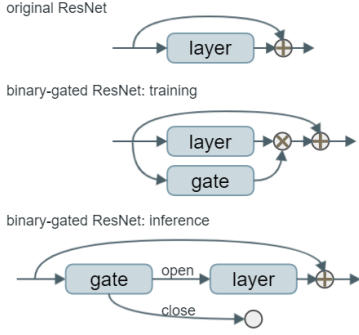


Figure 1: Illustration of a gating module with binary decision into the original residual model. In training, the learnable gating modules are trained as other parts of the network. At inference, the gate decisions are pre-loaded, and only the network parameters whose gate decision is open are loaded and computed.

where the insensitive state is triggered when $|x| > 1$. This is to avoid a possible scenario where a large gradient makes the STE output value stay at either 1 or 0 permanently.

An immediately observable advantage of the STE as the gating head is that it is a lightweight module for both forward and backward propagation. In the forward pass, no other computation than a sign check is needed. In the backward pass no computation needed. The gradient estimation, often viewed as a coarse approximation of the true gradient under noise, has been proved to positively correlate with the population gradient, and therefore gradient descent helps to minimize the empirical loss [Yin *et al.*, 2019].

4.3 Polarisation Regularizer

During the dynamic-pruning-style training, the matrix $\mathbf{W}_e(x)$ might not be the same for all $x \in \mathcal{X}$. To encourage a unified edge activation matrix that $\mathbf{W}_e(x) = \mathbf{W}_e(x'), \forall x, x' \in \mathcal{X}$, we introduce a polarisation regularizer $\mathcal{R}_{polar}(\{\mathbf{W}_e(x) | x \in \mathcal{X}\})$.

The complete loss function is:

$$\mathcal{L}(f(\mathbf{x}), \mathbf{y}) = \mathcal{L}_{task}(f(\mathbf{x}), \mathbf{y}) + \lambda \mathcal{R}_{polar}(\mathbf{W}_e(\mathbf{x})) \quad (6)$$

where \mathcal{L}_{task} is the task loss, *e.g.* cross-entropy loss for classification tasks and mean-squared error for regression tasks, and λ is the scale factor for polarisation regularizer.

The general form of $\mathcal{R}_{polar}(\mathbf{W}_e(\mathbf{x}))$ is in the form of an inverted parabola. Supposing $\mathbf{W}_e(x) \in \mathbb{R}^{|\mathcal{C}|}$ is flattened for all covered connections $c \in \mathcal{C}$:

$$\mathcal{R}_{polar}(\mathbf{W}_e(\mathbf{x})) := \frac{1}{|\mathcal{C}|} (\mathbf{1} - \bar{\mathbf{W}}_e(\mathbf{x}))^\top \bar{\mathbf{W}}_e(\mathbf{x}), \quad (7)$$

where $\bar{\mathbf{W}}_e(x) = \frac{1}{|\mathcal{X}|} \sum_{x \in \mathcal{X}} \mathbf{W}_e(x)$ is the averaged edge activation matrix over all data samples. Given the range of $\bar{\mathbf{W}}_{e,c} \in [0, 1]$, this form of inverted parabola ensures that an equivalent optimum can be reached when $\bar{\mathbf{W}}_{e,c}$ reaches either boundary of the range.

Specifically, in our ResNet layer-pruning scenario, the regularisation term is written as:

$$\mathcal{R}_{polar} := \frac{1}{|L|} \sum_{ly \in L} (1 - \bar{g}_{ly}) \bar{g}_{ly}, \quad (8)$$

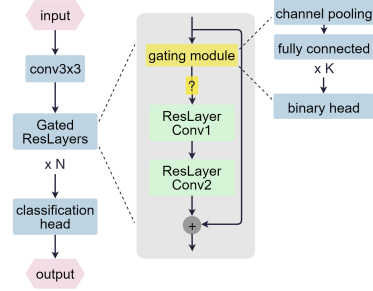


Figure 2: Illustration of layer-pruning gating modules in ResNet.

where $\bar{g}_{ly} = \frac{1}{|\mathcal{X}|} \sum_{x \in \mathcal{X}} g_{ly}(x) \in [0, 1]$ is the average of the gating module outputs over all input samples of the layer.

Similarly, in our ResNet channel-pruning scenario, the regularisation term is written as:

$$\mathcal{R}_{polar} := \frac{1}{|L|} \sum_{ly \in L} \frac{1}{|\mathcal{C}|} \sum_{ch \in \mathcal{C}} (1 - \bar{g}_{ly,ch}) \bar{g}_{ly,ch} \quad (9)$$

where $\bar{g}_{ly,ch} = \frac{1}{|\mathcal{X}|} \sum_{x \in \mathcal{X}} g_{ly,ch}(x) \in [0, 1]$ is the average of the gating module outputs over all input samples of the channel $ch \in \mathcal{C}$ in the layer $ly \in \mathcal{L}$.

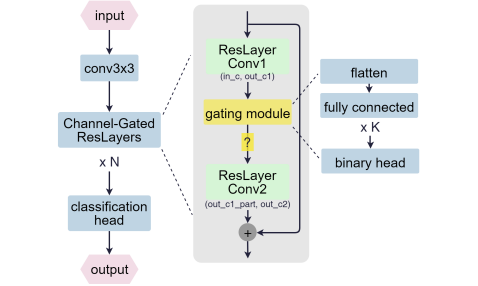
5 Experiments

5.1 Datasets and Architecture Specifications

We test the effectiveness of our proposed method on ResNet-110 [He *et al.*, 2015] as the full network. We chose CIFAR-10 and CIFAR-100 [Krizhevsky, 2009] as our datasets, which have widely-acknowledged test results on most variants of ResNets. Both datasets contain 50,000 images for training and 10,000 images for testing, both are 32x32 color images. The CIFAR-10 dataset has 10 classes, and CIFAR-100 has 100 classes. Testing both datasets show the effectiveness of our method under both simple and complex data distributions.

ResNet-110 has 54 residual layers, each consisting of 2 convolution layers. In layer pruning, we add the gating module at the beginning of each residual layer to decide whether the layer is to be computed or not. Figure 2 shows the designed position of the layer gating module. In channel pruning, we experiment on two layer designs and three positions of the gating module, and select the one with the best performance on test set. Figure 3 shows the three possible positions of the gating module. Table 1 shows the detailed design of the gating module.

Our experiments are conducted on one NVIDIA T4 GPU with 16GB Memory. The batch size is set to 256 for CIFAR-10 and 64 for CIFAR-100. Our training is done under a staged decaying learning rate for 350 epochs (although convergence can usually be achieved before 250 epochs.) The initial learning rate for both dataset is 0.1, and at each next stage will decrease to 10%. On CIFAR-10, the learning rate is adjusted at epochs 60, 120, and 160. On CIFAR-100, the learning rate is adjusted at epochs 125, 190, and 250. We chose stochastic gradient descent (SGD) as the optimizer, with a momentum of 0.9 and a weight decay of 5×10^{-4} . The networks and training



(a) Channel pruning between two convolutional layers.



(b) Channel pruning before the first convolution layer.

(c) Channel pruning after the second convolution layer.

Figure 3: Illustration of channel-pruning gating modules in ResNet: The gating module (a) between two convolutional layers; (b) before the first convolution layer; (c) after the second convolution layer. $K=1$ or 2 in our experiments.

procedures are implemented in PyTorch. When randomness is involved, we set the random seed to 1.

We apply the network to the image classification task. The pruned networks are evaluated by top-1 accuracy and FLOPs (floating-point operations). The FLOPs count is approximated by the `fvcore` package².

5.2 Pruning Results

Table 2 shows the results of the pruned networks on CIFAR-10 and CIFAR-100 datasets. It is easily observable that with the layer pruning scheme, we are able to save at least $\frac{1}{3}$ of computations (FLOPs) while sacrificing accuracy of less than 2%. Under the channel pruning scheme, we can save $\frac{1}{4}$ computations (FLOPs) while sacrificing accuracy of less than 3%.

In general, we note that the layer pruned models perform better than channel pruned models (i.e. there is a lower accuracy drop) for both CIFAR-10 and CIFAR-100, even when relative differences in FLOPs are taken into account. We believe this is because under the design of ResNet, the intermediate feature maps in each residual layer is sufficiently information-compact, and any removal on the feature maps can lead to information loss. The pruning ratio of channel pruning is positive though, with an almost 50% FLOPs reduction.

5.3 Comparison with Baselines

We compare its performance with naive baselines and other methods in the literature. For naive baselines, we consider

²<https://github.com/facebookresearch/fvcore>

Layer Gating Module	Channel Gating Module ($K=2$)
avg_pool_2d (output_size=channel_in)	flatten()
dense (in_dim=channel_in, out_dim=16)	dense(in_dim=out_channel*feature_size, out_dim=16)
batch_norm_1d()	batch_norm_1d()
ReLU()	ReLU()
dense (in_dim=16, out_dim=1)	dense(in_dim=16, out_dim=1)
STE()	STE()

Table 1: Layer and channel gating module design. **Left:** “channel_in” is the input channel number for the first convolution layer in the residual layer. **Right:** “mid_channel” is the output channel number for the first convolution layer, equal to the input channel number for the second convolution layer. “feature_size” is the dimension of a flattened feature map. For other K value, we simply vary the dense layer number.

the following:

- **Naive Dropout ResNet-56:** A standard classifier but with $k \in \{20\%, 30\%, 50\%, 60\%, 80\%\}$ parameters randomly pruned during testing.
- **Naive Layer Pruned ResNet-56:** The same classifier but with $k \in \{20\%, 30\%, 50\%, 60\%, 80\%\}$ layer activations randomly set to 0 during testing.

A visualized comparison with the naive baselines is shown in Figure 4, demonstrating our pruning method’s ability to maintain network performance with a high pruning ratio.

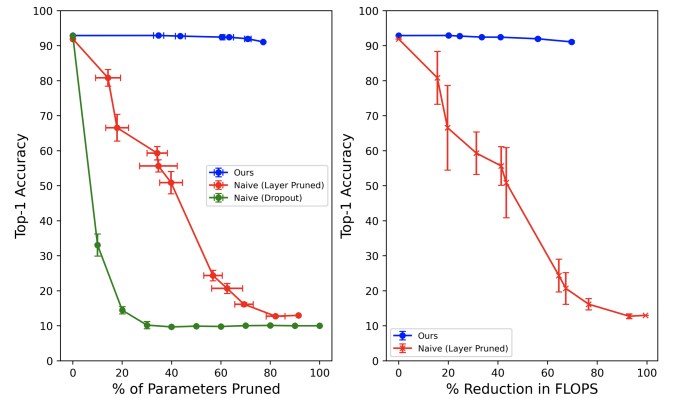


Figure 4: Comparison of our method with some naive baselines on CIFAR-10 with ResNet-56. **Left:** Pruning rate vs Top-1 accuracy. **Right:** % FLOPs reduction vs Top-1 accuracy. Here, the naive dropout method does not reduce FLOPs, so we omitted it.

For comparison, we consider the methods that also followed the idea of simultaneous pruning and learning, as listed in Table 3. Figure 5 shows the performance of our scheme against some methods found in literature, all of which use the ResNet-56 as the base network. We note that our scheme provides competitive results not only in terms of the absolute accuracy, but also the accuracy drop resulting from pruning. To better compare to these methods quantitatively at similar pruning rates, we control the pruning rate by an additional sparsity regularization term in the loss function that penalises

Dataset	Model	Top-1 accuracy (%)	Gate open ratio (%)	FLOPs (M)(rel)
CIFAR-10	baseline	93.68 (0)	100.00	255.3 (1)
	layer pruned	92.82 (-0.86)	53.70	137.7 (0.54)
	channel pruned	91.01 (-2.67)	48.76	189.9 (0.74)
CIFAR-100	baseline	71.85 (0)	100.00	255.3 (1)
	layer pruned	70.01 (-1.84)	66.67	171.1 (0.67)
	channel pruned	66.91 (-4.94)	51.14	135.41 (0.52)

Table 2: Results of pruned networks on CIFAR-10 and CIFAR-100 datasets. Numbers in brackets in top-1 accuracy shows the relative difference from the baseline model. FLOPs is counted in millions (M). Numbers in brackets in FLOPs shows the relative ratio from the baseline model. Baseline model is ResNet110.

Method	Unpruned Accuracy	Pruned Accuracy	% FLOPS Reduction	Accuracy Drop
Ours	93.43	92.42 \pm 0.14	41.81 \pm 4.01	1.01 \pm 0.14
AMC [He <i>et al.</i> , 2018b]	92.80	91.90	50.00	1.10
Importance [Dekhovitch <i>et al.</i> , 2021]	93.60	91.90	39.90	1.14
SFP [He <i>et al.</i> , 2018a]	93.59	92.26	52.60	1.33
CP [He <i>et al.</i> , 2017b]	92.80	91.80	50.00	1.00
PFEC [Li <i>et al.</i> , 2016b]	93.04	91.31	27.60	1.73
VCP [Zhao <i>et al.</i> , 2019]	93.04	92.26	20.30	0.78

Table 3: The performance of our method over 5 trials against some established, related methods in literature for $\approx 50\%$ FLOPs reduction (**Dataset**: CIFAR-10, **Model**: ResNet-56). We note that our method offers a competitive trade-off between accuracy and FLOPs while being simple to implement. For SFP, we consider only the pre-trained variant for fair comparison as the fine-tuning variant in the paper incurs extra computational costs that are not necessarily considered.

non-zero activations. The resulting loss function is:

$$\mathcal{L}(f(\mathbf{x}), \mathbf{y}) = \mathcal{L}_{task}(f(\mathbf{x}), \mathbf{y}) + \lambda_{polar} \mathcal{R}_{polar}(\mathbf{W}_e(\mathbf{x})) + \lambda_{act} \mathcal{R}_{act}(\mathbf{W}_e(\mathbf{x})) \quad (10)$$

where

$$\mathcal{R}_{act}(\mathbf{W}_e(\mathbf{x})) = \frac{1}{|L|} \sum_{l_y \in L} \bar{g}_{l_y} \quad (11)$$

is the overall average layer activation, where the average is taken across layers $l_y \in \mathcal{L}$ and inputs $x \in \mathcal{X}$. We now set $\lambda_{polar} = 1$, the gating function as Gumbel-softmax, and vary $\lambda_{act} \in [0, 1]$ to change the pruning rate.

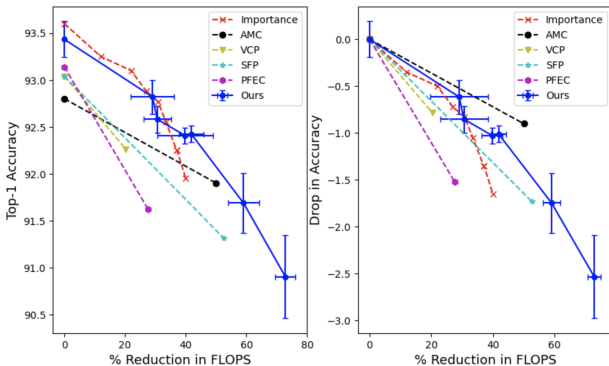


Figure 5: Comparison between our scheme and related methods in literature on CIFAR-10 with ResNet-56. **Left**: Pruning rate vs Top-1 accuracy. **Right**: % FLOPs reduction vs Top-1 accuracy drop.

Function	Top-1 accuracy (%)	\mathcal{R}_{polar}
STE	92.86	0.00
Gumbel-softmax	94.05	0.0039
Bernoulli	91.96	0.2454

Table 4: Results of different gating functions on CIFAR-10. \mathcal{R}_{polar} taken at the end of training session, each with the same number of epochs. A larger \mathcal{R}_{polar} corresponds to a less unified sub-networks after convergence (not ideal). These experiments were performed on ResNet110 with $\lambda_{polar} = 3$.

5.4 Ablation Studies

We test the individual utility of the two major modules, STE and polarisation regularizer, through ablation studies. To test the utility of STE, we replace STE with sampling from Bernoulli distribution and with Gumbel-softmax. When sampling from Bernoulli distribution, we set up a threshold equal to the mean of the gating module’s outputs right after the last dense layer (*i.e.* right before the original STE). If the output is larger than the mean, we keep the layer; Otherwise we prune the layer. Table 4 shows results from the three gating functions, experimented on CIFAR-10. We observed that other than STE, no other gating head function can result in a perfectly unified and stable sub-network. We can thus conclude on the utility of STE in terms of stabilising on the dynamic sub-networks and keeping the expected performances. However, we should also note that the Gumbel-softmax has the potential to achieve a better task performance while keeping a set of merely lightly dynamic sub-networks indicated from the low level of \mathcal{R}_{polar} . The discussion should then be open that, whether a suitable unification tweak on the resul-

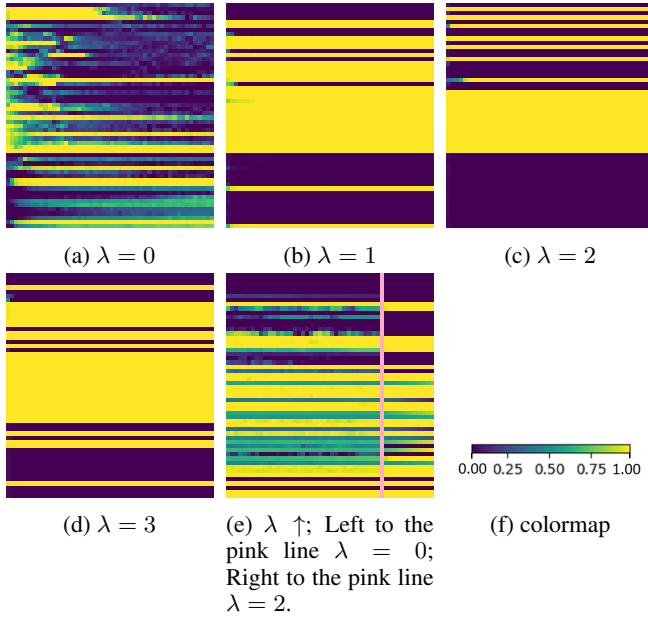


Figure 6: Layer opening ratio during training under different λ values. Each row represents one layer among the 54 layers. Each column corresponds to one epoch. For $\lambda \in \{0, 1, 2, 3\}$, we include the first 50 training epochs. For $\lambda \uparrow$, we take the part before and after the λ change (separated by the pink line).

Spec	Top-1 accuracy (%) (rel)	gate open ratio (%)
baseline	93.68 (0)	100.00
$\lambda_{polar} = 0$	90.79 (-2.89)	18.52 - 53.70
$\lambda_{polar} = 1$	92.44 (-1.24)	53.70
$\lambda_{polar} = 2$	91.67 (-2.01)	40.74
$\lambda_{polar} = 3$	91.85 (-1.83)	57.41
$\lambda_{polar} \uparrow$	93.18 (-0.50)	55.56

Table 5: Results of pruned networks under different λ_{polar} values on CIFAR-10 (ResNet110). " $\lambda_{polar} \uparrow$ " uses the settings of $\lambda_{polar} = 0$ for the first 125 epochs; $\lambda = 2$ for the next 65 epochs; and $\lambda = 3$ for the resting epochs until end of training.

tant dynamic sub-networks from Gumbel-softmax can further improve the performances that STE can reach.

To test the utility of polarisation regularizer, we experimented on a series of λ_{polar} values, from 0 to 3. We also experimented on the effect of gradually increasing regularizer weight λ_{polar} during a training session in order to verify whether a partially trained network would affect the pruning results. Figure 6 shows the layer pruning evolution under different λ_{polar} settings and Table 5 shows the performance of the resulting sub-networks. The layer pruning evolutions show that as λ_{polar} increases, the convergence to a unified sub-network is accelerated. Figure 6e demonstrates a clear evolution pattern before and after λ_{polar} turned on. We thus can conclude on the individual effect of the polarisation regularization. The test set results, however, show no clear correlation between λ_{polar} value and the resultant accuracy or gate open ratio. Therefore, the selection of λ_{polar} can be mostly determined via empirical results.

Model	top-1 accuracy (%) (rel)	gate open ratio (%)
baseline	93.68 (0)	100.00
1FC-before	69.71 (-23.97)	47.82
1FC-middle	90.60 (-3.08)	47.77
1FC-after	83.89 (-9.79)	41.91
2FC-before	85.39 (-8.29)	48.93
2FC-middle	82.94 (-10.74)	49.36
2FC-after	91.01 (-2.67)	48.76

Table 6: Channel pruning results under different gating module specifications on CIFAR-10 dataset. Numbers in brackets in top-1 accuracy shows the relative difference (rel) from the baseline model. "NFC" refers to $N = \{1, 2\}$ dense layer(s) in gating module and "before", "middle", and "after" for the three gating module positions, illustrated in Figure 3.

5.5 Channel Pruning Design Choices

We tested multiple channel pruning designs and selected the one with the most outstanding performances in classification accuracy and channel pruning ratio. Table 6 shows the pruning results under different gating module architectures and positions, tested on CIFAR-10. For gating module architectures (recall Table 1), we experimented on one dense layers and two dense layers. For gating module positions (recall Figure 3), we experimented on the gating module in front of each residual layer, in the middle of two convolution layers in a residual layer, and at the end of each residual layer. On CIFAR-10, results show that while all designs achieve a similar channel pruning ratio, the design with 2 dense layers and placed at the end of each residual layer (2FC-after) achieves the best classification accuracy that is significantly higher than most others. However, the design with 1 dense layer placed between two convolution layers (1FC-middle) also achieves a similar accuracy.

6 Conclusion

We proposed a network pruning scheme that maintains performance while being more computationally efficient (thus greener). Through simultaneous parameter and structure optimization, our pruning scheme finds a stable sub-network with similar performances on the same downstream task as the full network. The scheme consists of a differentiable, lightweight binary gating module and novel regularisers to enforce unification (data-invariance) of the pruned sub-networks. Experiments on two types of pruned network elements (layer and channel) show that the scheme can find sub-networks with significant reduction in FLOPs (>50%) with minimal sacrifice in downstream performance (<1%). Compared to other similar methods, the sub-network's accuracy and accuracy drop from our method are among the best. With fine tuning of our uncovered sub-networks, we anticipate further performance improvements - however, this is beyond the scope of our work, which aims to emphasise maximal performance gains within limited computational budgets. Beyond convolutional networks, we look forward to testing the applicability of our pruning scheme to other base networks, datasets and tasks. We hope that our encouraging results facilitate the transition towards energy efficient deep learning models.

References

- [Bejnordi *et al.*, 2019] Babak Ehteshami Bejnordi, Tijmen Blankevoort, and Max Welling. Batch-shaping for learning conditional channel gated networks, 2019.
- [Bengio *et al.*, 2013] Yoshua Bengio, Nicholas Léonard, and Aaron Courville. Estimating or propagating gradients through stochastic neurons for conditional computation, 2013.
- [Cai *et al.*, 2019] Han Cai, Chuang Gan, Tianzhe Wang, Zhekai Zhang, and Song Han. Once-for-all: Train one network and specialize it for efficient deployment, 2019.
- [Chang *et al.*, 2019] Jianlong Chang, Xinbang Zhang, Yiwen Guo, Gaofeng Meng, Shiming Xiang, and Chunhong Pan. Differentiable architecture search with ensemble gumbel-softmax, 2019.
- [Cheong, 2019] Robin Cheong. transformers . zip : Compressing transformers with pruning and quantization. 2019.
- [Dekhovitch *et al.*, 2021] Aleksandr Dekhovitch, David M. J. Tax, Marcel H. F. Sluiter, and Miguel A. Bessa. Neural network relief: a pruning algorithm based on neural activity. *CoRR*, abs/2109.10795, 2021.
- [Denil *et al.*, 2013] Misha Denil, Babak Shakibi, Laurent Dinh, Marc’Aurelio Ranzato, and Nando de Freitas. Predicting parameters in deep learning, 2013.
- [Dodge *et al.*, 2022] Jesse Dodge, Taylor Prewitt, Remi Tachet Des Combes, Erika Odmark, Roy Schwartz, Emma Strubell, Alexandra Sasha Luccioni, Noah A. Smith, Nicole DeCario, and Will Buchanan. Measuring the carbon intensity of ai in cloud instances, 2022.
- [Dosovitskiy *et al.*, 2020] Alexey Dosovitskiy, Lucas Beyer, Alexander Kolesnikov, Dirk Weissenborn, Xiaohua Zhai, Thomas Unterthiner, Mostafa Dehghani, Matthias Minderer, Georg Heigold, Sylvain Gelly, Jakob Uszkoreit, and Neil Houlsby. An image is worth 16x16 words: Transformers for image recognition at scale, 2020.
- [EIA US, 2021] EIA US. 2020 average monthly bill- residential. https://www.eia.gov/electricity/sales_revenue_price/pdf/table5_a.pdf, 2021. Accessed: 2022-07-19.
- [Frankle and Carbin, 2019] Jonathan Frankle and Michael Carbin. The lottery ticket hypothesis: Finding sparse, trainable neural networks. In *7th International Conference on Learning Representations, ICLR 2019, New Orleans, LA, USA, May 6-9, 2019*. OpenReview.net, 2019.
- [Gao *et al.*, 2018] Xitong Gao, Yiren Zhao, Łukasz Dudziak, Robert Mullins, and Cheng-zhong Xu. Dynamic channel pruning: Feature boosting and suppression, 2018.
- [Gholami *et al.*, 2021] Amir Gholami, Sehoon Kim, Zhen Dong, Zhewei Yao, Michael W. Mahoney, and Kurt Keutzer. A survey of quantization methods for efficient neural network inference, 2021.
- [Han *et al.*, 2015] Song Han, Jeff Pool, John Tran, and William J. Dally. Learning both weights and connections for efficient neural networks, 2015.
- [He *et al.*, 2015] Kaiming He, Xiangyu Zhang, Shaoqing Ren, and Jian Sun. Deep residual learning for image recognition, 2015.
- [He *et al.*, 2017a] Yihui He, Xiangyu Zhang, and Jian Sun. Channel pruning for accelerating very deep neural networks, 2017.
- [He *et al.*, 2017b] Yihui He, Xiangyu Zhang, and Jian Sun. Channel pruning for accelerating very deep neural networks. In *2017 IEEE International Conference on Computer Vision (ICCV)*, pages 1398–1406, 2017.
- [He *et al.*, 2018a] Yang He, Guoliang Kang, Xuanyi Dong, Yanwei Fu, and Yi Yang. Soft filter pruning for accelerating deep convolutional neural networks. In *International Joint Conference on Artificial Intelligence (IJCAI)*, pages 2234–2240, 2018.
- [He *et al.*, 2018b] Yihui He, Ji Lin, Zhijian Liu, Hanrui Wang, Li-Jia Li, and Song Han. AMC: AutoML for model compression and acceleration on mobile devices. In *Computer Vision – ECCV 2018*, pages 815–832. Springer International Publishing, 2018.
- [Hinton *et al.*, 2015] Geoffrey Hinton, Oriol Vinyals, and Jeff Dean. Distilling the knowledge in a neural network, 2015.
- [Hou *et al.*, 2022] Zejiang Hou, Minghai Qin, Fei Sun, Xiaolong Ma, Kun Yuan, Yi Xu, Yen-Kuang Chen, Rong Jin, Yuan Xie, and Sun-Yuan Kung. Chex: Channel exploration for cnn model compression, 2022.
- [Jang *et al.*, 2016] Eric Jang, Shixiang Gu, and Ben Poole. Categorical reparameterization with gumbel-softmax, 2016.
- [Jouppi *et al.*, 2020] Norman P. Jouppi, Doe Hyun Yoon, George Kurian, Sheng Li, Nishant Patil, James Laudon, Cliff Young, and David Patterson. A domain-specific supercomputer for training deep neural networks. *Commun. ACM*, 63(7):67–78, jun 2020.
- [Krizhevsky, 2009] Alex Krizhevsky. Learning multiple layers of features from tiny images. Technical report, 2009.
- [Kusner and Hernández-Lobato, 2016] Matt J. Kusner and José Miguel Hernández-Lobato. Gans for sequences of discrete elements with the gumbel-softmax distribution, 2016.
- [Lee *et al.*, 2018] Namhoon Lee, Thalaiyasingam Ajanthan, and Philip H. S. Torr. Snip: Single-shot network pruning based on connection sensitivity, 2018.
- [Lee, 2019] Yognjin Lee. Differentiable sparsification for deep neural networks, 2019.
- [Li *et al.*, 2016a] Hao Li, Asim Kadav, Igor Durdanovic, Hanan Samet, and Hans Peter Graf. Pruning filters for efficient convnets, 2016.
- [Li *et al.*, 2016b] Hao Li, Asim Kadav, Igor Durdanovic, Hanan Samet, and Hans Peter Graf. Pruning filters for efficient convnets. *ArXiv*, abs/1608.08710, 2016.
- [Li *et al.*, 2020] Yawei Li, Shuhang Gu, Christoph Mayer, Luc Van Gool, and Radu Timofte. Group sparsity: The

- hinge between filter pruning and decomposition for network compression, 2020.
- [Lin *et al.*, 2017] Ji Lin, Yongming Rao, Jiwen Lu, and Jie Zhou. Runtime neural pruning. In I. Guyon, U. Von Luxburg, S. Bengio, H. Wallach, R. Fergus, S. Vishwanathan, and R. Garnett, editors, *Advances in Neural Information Processing Systems*, volume 30. Curran Associates, Inc., 2017.
- [Lin *et al.*, 2019] Shaohui Lin, Rongrong Ji, Yuchao Li, Cheng Deng, and Xuelong Li. Towards compact convnets via structure-sparsity regularized filter pruning, 2019.
- [Lin *et al.*, 2020] Zi Lin, Jeremiah Liu, Zi Yang, Nan Hua, and Dan Roth. Pruning redundant mappings in transformer models via spectral-normalized identity prior. In *Findings of the Association for Computational Linguistics: EMNLP 2020*, pages 719–730, Online, November 2020. Association for Computational Linguistics.
- [Luo *et al.*, 2019] J. Luo, H. Zhang, H. Zhou, C. Xie, J. Wu, and W. Lin. Thinet: Pruning cnn filters for a thinner net. *IEEE Transactions on Pattern Analysis & Machine Intelligence*, 41(10):2525–2538, oct 2019.
- [Patterson *et al.*, 2021] David Patterson, Joseph Gonzalez, Quoc Le, Chen Liang, Lluís-Miquel Munguia, Daniel Rothchild, David So, Maud Texier, and Jeff Dean. Carbon emissions and large neural network training, 2021.
- [Ramanujan *et al.*, 2019] Vivek Ramanujan, Mitchell Wortsman, Aniruddha Kembhavi, Ali Farhadi, and Mohammad Rastegari. What’s hidden in a randomly weighted neural network?, 2019.
- [Schwartz *et al.*, 2020] Roy Schwartz, Jesse Dodge, Noah A. Smith, and Oren Etzioni. Green ai. *Commun. ACM*, 63(12):54–63, nov 2020.
- [Shafiee *et al.*, 2018] Mohammad Saeed Shafiee, Mohammad Javad Shafiee, and Alexander Wong. Dynamic representations toward efficient inference on deep neural networks by decision gates, 2018.
- [Shen *et al.*, 2021] Jiayi Shen, Xiantong Zhen, Marcel Worring, and Ling Shao. Variational multi-task learning with gumbel-softmax priors. In M. Ranzato, A. Beygelzimer, Y. Dauphin, P.S. Liang, and J. Wortman Vaughan, editors, *Advances in Neural Information Processing Systems*, volume 34, pages 21031–21042. Curran Associates, Inc., 2021.
- [Srinivas and Babu, 2015] Suraj Srinivas and R. Venkatesh Babu. Learning neural network architectures using back-propagation, 2015.
- [Veit and Belongie, 2017] Andreas Veit and Serge Belongie. Convolutional networks with adaptive inference graphs, 2017.
- [Wortsman *et al.*, 2019] Mitchell Wortsman, Ali Farhadi, and Mohammad Rastegari. Discovering neural wirings, 2019.
- [Yin *et al.*, 2019] Penghang Yin, Jiancheng Lyu, Shuai Zhang, Stanley Osher, Yingyong Qi, and Jack Xin. Understanding straight-through estimator in training activation quantized neural nets, 2019.
- [Yin *et al.*, 2021] Hongxu Yin, Arash Vahdat, Jose Alvarez, Arun Mallya, Jan Kautz, and Pavlo Molchanov. A-vit: Adaptive tokens for efficient vision transformer, 2021.
- [Zhang and Stadie, 2019] Matthew Shunshi Zhang and Bradley Stadie. One-shot pruning of recurrent neural networks by jacobian spectrum evaluation, 2019.
- [Zhao *et al.*, 2019] Chenglong Zhao, Bingbing Ni, Jian Zhang, Qiwei Zhao, Wenjun Zhang, and Qi Tian. Variational convolutional neural network pruning. In *2019 IEEE/CVF Conference on Computer Vision and Pattern Recognition (CVPR)*, pages 2775–2784, 2019.
- [Zhu *et al.*, 2021] Mingjian Zhu, Yehui Tang, and Kai Han. Vision transformer pruning, 2021.
- [Zhuang *et al.*, 2020] Tao Zhuang, Zhixuan Zhang, Yuheng Huang, Xiaoyi Zeng, Kai Shuang, and Xiang Li. Neuron-level structured pruning using polarization regularizer. In H. Larochelle, M. Ranzato, R. Hadsell, M.F. Balcan, and H. Lin, editors, *Advances in Neural Information Processing Systems*, volume 33, pages 9865–9877. Curran Associates, Inc., 2020.